Experiments in Fluids 8, 77–85 (1989)

Experiments in Fluids

Mean flow characteristics of a turbulent plane jet with buoyancy induced curvature

G. J. Hitchman, A. A. Abdel-Rahman*, P. R. Slawson and **A. B. Strong**

Dept. of Mechanical Engineering, University of Waterloo, Waterloo, Ontario N2L 3G1, Canada

Abstract. An experimental investigation of heated vertical and inclined plane air jets discharged into quiescent surroundings is described. A unique feature of this data is that Pitot tube measurements were used to define the mean trajectory of the inclined jets so that subsequent hot-wire traverses could be made normal to the curved path. While the mean velocity and temperature profiles are self-similar for the range of exit conditions studied, other aspects of the mean jet development depend on the exit Reynolds and Froude numbers, or the discharge angle. It is noted that variations between this study and other published data suggest further measurements of this flow situation are needed, with particular attention to specific features of the jet apparatus and ambient surroundings, and to the exit Reynolds number.

List of symbols

b	half-width
C, C_0, C^*	constants defining decay rates
D	exit width of the jet
Fr	jet exit densimetric Froude number ($\varrho_0 U_0/g D \Delta\varrho_0$)
I	velocity profile integral parameter
K, K_0	constants defining spread rates
M	momentum flux
Re	jet exit Reynolds number
s, n	curvilinear axes of the jet flow
T	temperature
U, V	streamwise and transverse velocity
U_s	velocity scale [Eq. (3)]
x_1	length scale [Eq. (4)]
x, y, z	Cartesian axes of the jet flow
ΔT	excess temperature ($T-T_a$)
θ	jet discharge angle relative to vertical ($\theta=0°$)
η	y/b or n/b
ϕ	momentum thickness of the nozzle boundary layer
ϱ	air density

Subscripts

a	ambient
c	jet centerline
0	jet exit
t	refers to temperature
u	refers to velocity
∞	refers to far field
overbar	time average

* Presently with Dept. of Mechanical Engineering, University of Alexandria, Alexandria, Egypt

1 Introduction

Most of the experimental work on the effects of streamline curvature on the structure of turbulent flows has focussed on solid boundary pressure induced curvature (e.g. Pelfrey and Liburdy 1986). The resulting turbulent flow over a curved boundary, e.g., experiences stabilizing effects if the surface is concave or destabilizing effects if the surface is convex. By comparison, relatively little experimental data exists on the effects of buoyancy induced curvature on the character of free turbulent shear flows (e.g. Lemieux 1983). Here, both buoyancy and curvature effects are present and may result in competing influences. For example, the heated inclined plane jet shown in Fig. 1 is thermally stable on the convex (lower) side, and unstable on the concave (upper) side, while dynamically the flow (due to curvature) is stable on the concave side and unstable on the convex side (Bradshaw 1973). The present study investigates and attempts to elucidate both buoyant and curvature stability effects on the mean (time averaged) characteristics of a heated inclined plane jet issued into a quiescent medium. Of particular interest is the symmetry and growth aspects of the mean velocity and excess temperature profiles across the jet as a function of the distance along the centerline.

The buoyant round or slot jet discharged horizontally or at arbitrary angles into quiescent surroundings has been studied theoretically and or experimentally by Abraham (1963, 1965), Anwar (1969), Fan and Brooks (1969), Cederwall (1971), Chan and Kennedy (1972) and Lemieux (1983). Cederwall (1971) conducted experiments on a buoyant slot jet discharged horizontally into quiescent surroundings and found resonable agreement between his mean jet characteristics and the integral predictions of Abraham (1963) and Fan and Brooks (1969). The integral model of Chan and Kennedy (1972) also reasonably predicts the results of Cederwall (1971). Lemieux (1983) conducted an experimental study on both the mean and turbulence structure of a heated slot jet discharged at four angles including the vertical and horizontal cases. He reports only limited success in predicting the experimental trajectory of his horizontally

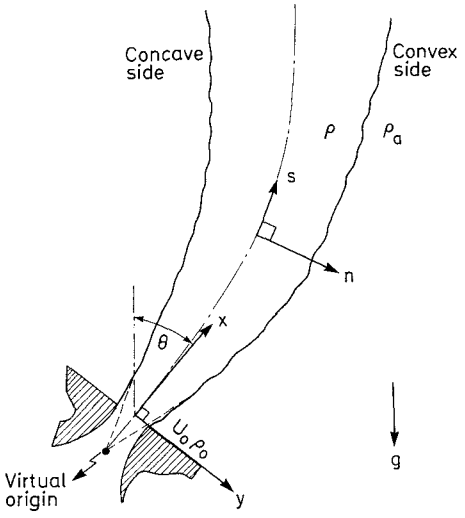

Fig. 1. Definition sketch of the heated inclined plane jet

released jet using either his or Chan and Kennedy's (1972) integral model. In summarizing the development of the jet, Lemieux reports that the mean velocity and temperature profiles were self-similar in the far field except for a slight asymmetry in the inclined jets which he attributed to the thermal stability effects. The rate of spread of temperature was greater than that of velocity, with both being essentially independent of the range of buoyancy and discharge angles tested, but dependent on *Re*. He found that the rate of decay of centerline temperature was greater than that of velocity with both being dependent on buoyancy. However, the rate of decay of temperature was also dependent on the discharge angle.

The study by Lemieux provides an excellent data base for comparison with the present results. Before a detailed comparison can be made however, any differences in experimental setup and technique and their effect on the respective results must be considered. Both studies used an X-array hot-wire anemometry technique. Lemieux's X-wire traverses were made normal to the jet discharge direction, rather than the trajectory as in the present study, with the result that only the x-component of the streamwise velocity was measured. His traversing method creates a misalignment between the probe axis and the local mean flow direction, thereby introducing a source of error associated with the yaw sensitivity of the X-wire. Lemieux analysed his X-wire signals using the cosine cooling law which is not recommended for flows of low velocities or high turbulence levels (e.g. Champagne et al. 1967; Bruun 1972; Bruun and Tropea 1985), while in this study a comprehensive technique incorporating both yaw and temperature sensitivities was used (Abdel-Rahman et al. 1988a). Lemieux conducted his experiments with a fixed exit velocity U_0 but changed his jet exit excess temperature $\Delta\overline{T}_0$ giving *Fr*'s of 715 and 1430, and *Re*'s of 1500 and 1700 which resulted in density ratios $\varrho_a/\varrho_0 \approx 1.06$ and 1.14. In the present study $\Delta\overline{T}_0$, and hence ϱ_a/ϱ_0, was held constant at ≈ 1.25 while a change in *Fr* between 800 and 1450 was achieved by changing U_0 resulting in *Re*'s of 1880 and 2600. Chen and Rodi (1980) report a significant influence of ϱ_a/ϱ_0 on the rates of decay and spread in plane jets. However, Lemieux and Oosthuizen (1984) and Otugen and Namer (1986) have shown that the development of the plane jet is also influenced by *Re*, particularly in the range of these experiments. Other differences between this study and Lemieux's will be discussed within the context of interpreting the results.

The overall objective of the current research is to further the understanding of free shear flows with buoyancy induced curvature, and ultimately, to provide experimental data to aid in the development of prediction methods. A primary objective of the present work was to provide a detailed data base to support and extend the results of Lemieux (1983). To this end, preliminary Pitot tube measurements were used to define the curved path of the heated inclined jets after which detailed profile measurements were made normal to the jet trajectory using the X-wire probe.

2 Experimental design and procedure

The jet apparatus, originally constructed by Reardon (1985), now consists of a variable speed centrifugal blower which supplies the air through a 3.7 m long round flexible duct and a 1.0 m diffuser section, to a 400 mm × 600 mm × 125 mm settling chamber, followed by a corner section containing 90° turning vanes, a second shorter settling chamber, and finally a 40 : 1 contraction which ends as a 600 mm × 10 mm slot. The jet issues from a floor which spans the length of the slot and extends 300 mm on each side. The jet is confined by two vertical walls which extent 1200 mm on the upper and 1000 mm on the lower side of the slot. The entrained air passes through 0.8 open-air ratio screens spanning the ends of the confining walls. Profile measurements of the mean velocity and turbulence intensity ($<0.7\%$) at the nozzle exit indicate that the initial wall boundary layers are laminar. The jet flow can be uniformly heated to a maximum excess temperature of $\approx 80\,^{\circ}\mathrm{C}$, and maintained constant to within $\pm 1\,^{\circ}\mathrm{C}$, at a nominal exit velocity of 4.0 m/s. The measuring probes are moved in the s, n plane (Fig. 1) to within 0.01 mm by a micro-computer controlled traversing mechanism.

Preliminary profile measurements and two-dimensionality checks were made with a Pitot tube and a 5 μm cold-wire probe. The detailed profile measurements were made with a triple-wire probe comprising a DISA 55P51 gold-plated tungsten X-wire connected to a DISA 56C01 system through two 56C16 general purpose bridges and a 1 μm platinum wire operated in constant current mode using a 56C20 temperature bridge. The three analog signals from the triple-wire probe were simultaneously sampled using a multichannel, high speed, 12 bit A/D converter interfaced under DMA control to an IBM PC-XT.

The digitized hot-wire signals were interpreted using the response equation given by Collis and Williams (1959) be-

Table 1. Spread and decay constants for velocity and excess temperature

Experiment code and conditions	K_u [a]	K_t [a]	K_t [b]	C_u [a]	C_u^*	C_t [c]
A1 ($Fr=1456$, $Re=2585$, $\theta=0.0°$)	0.129	0.134	0.134	0.185	0.219	0.413
B1 ($Fr=1451$, $Re=2601$, $\theta=22.5°$)	0.128	0.144	0.143	0.126	0.195	0.360
C1 ($Fr=1453$, $Re=2560$, $\theta=45.0°$)	0.123	0.155	0.136	0.128	0.184	0.373
A2 ($Fr=805$, $Re=1879$, $\theta=0.0°$)	0.159	0.166	0.166	0.122	0.212	0.429
B2 ($Fr=792$, $Re=1878$, $\theta=22.5°$)	0.132	0.137	0.149	0.091	0.165	0.395
C2 ($Fr=790$, $Re=1913$, $\theta=45.0°$)	0.138	0.154	0.145	0.100	0.180	0.391
Lemieux ($Fr=715$, $Re=1500$, $\theta=0.0°$)	0.121	0.136	0.132	0.211	0.178	0.400
Lemieux ($Fr=715$, $Re=1500$, $\theta=30.0°$)	–	–	–	–	–	0.402
R & C: 1985 ($Fr=110$, $Re=1600$, $\theta=0.0°$)	0.112	–	0.167	0.093	0.168	0.194

[a] $15 \geq s/D \leq 75$
[b] $15 \geq s/D \leq 50$
[c] $5 \geq s/D \leq 30$

cause it represents a physical heat transfer model for the hot-wire, rather than just a regression model, and thus, inherently accounts for the complete separation of temperature and velocity effects on the hot-wire signals (Abdel-Rahman et al. 1988a). Bruun and Tropea (1985) recommended that a digital technique incorporating the yaw dependence of all the calibration coefficients should be used when instantaneous velocity components are desired. Reardon (1985) developed a technique similar to theirs and it has been extended for use in the present study (Abdel-Rahman et al. 1988a).

The heated jet flow was studied at discharge angles $\theta=0$, 22.5 and 45°. For each θ, experiments were conducted at $Fr \approx 800$ and 1450, which correspond to $U_0 \approx 4.5$ and 6.2 m/s, $Re \approx 1880$ and 2600 and a constant $\varrho_a/\varrho_0 \approx 1.25$. The loci of the positions of maximum velocity from profiles made normal to the axis of discharge of the inclined jets (y-direction) using a Pitot tube and cold-wire defined the curved trajectory of the jet for each of four combinations of θ and Fr. From these trajectories, the appropriate traverse lines in the n-direction were calculated for the subsequent detailed measurements using the triple-wire probe. Lateral profiles of $\bar{U}$, $\bar{V}$, and $\Delta\bar{T}$ were measured at up to seven downstream stations out to 75 nozzle widths (s/D) for six experimental conditions as defined in Table 1. The estimated uncertainties associated with the measured quantities are: $\bar{U} \pm 2.0\%$; $\bar{V} \pm 3.0\%$; $\Delta\bar{T} \pm 1.5\%$ (Abdel-Rahman 1987).

3 Results and discussion

3.1 Jet trajectory

The jet trajectories for the four inclined cases are shown in Fig. 2 each plotted with respect to their initial angle of discharge θ. Significant buoyancy-induced displacements of the jet's centerline with respect to θ are evident. The displacement of case C2 at $s/D=60$ exceeds that found by Lemieux (1983) by about a factor of two for similar jet exit conditions. Possible reasons for this discrepancy will be discussed later in the paper. Jet trajectories based on the temperature field were found to be similar but slightly above those of the velocity field. All subsequent data are analyzed with respect to the velocity centerline.

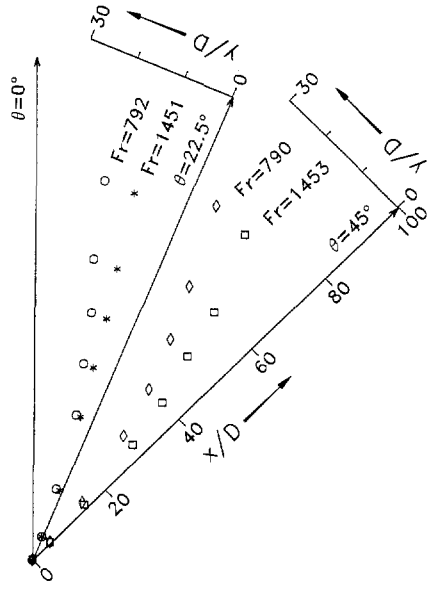

Fig. 2. Effect of θ and Fr on jet trajectory; * – B1; o – B2; □ – C1; ◇ – C2

3.2 Mean streamwise velocity and excess temperature

The profiles of mean streamwise velocity $\bar{U}/U_0$ for the higher Fr experiments shown in Fig. 3b indicate that velocities in the central portion of the jet are slightly lower in the vertical jet (A1) compared to the inclined jets (B1 and C1), a trend which was evident in the lower Fr data as well. Figure 3b also illustrates that increasing the Re and Fr for a fixed θ slightly increases $\bar{U}/U_0$ (C1 versus C2). Lemieux's (1983) measured x-component of $\bar{U}$ was sensitive to changes in Fr and θ but in both cases the trends were opposite to those described above. These differences in behaviour might be related to the variations in Re and or the greater degree of curvature found here which implies generally lower rates of dilution relative to Lemieux's results.

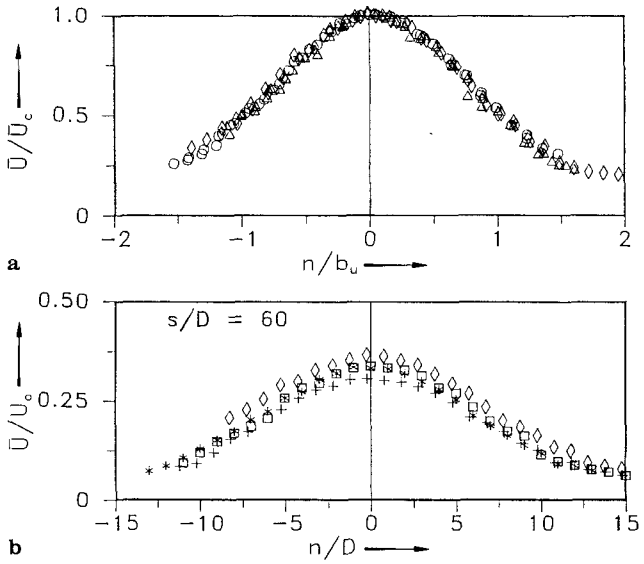

Fig. 3a and b. Profiles of streamwise mean velocity normalized by **a** $\bar{U}_c$ and b_u, and **b** U_0 and D; + – A1; △ – A2; * – B1; ○ – B2; □ – C1; ◇ – C2

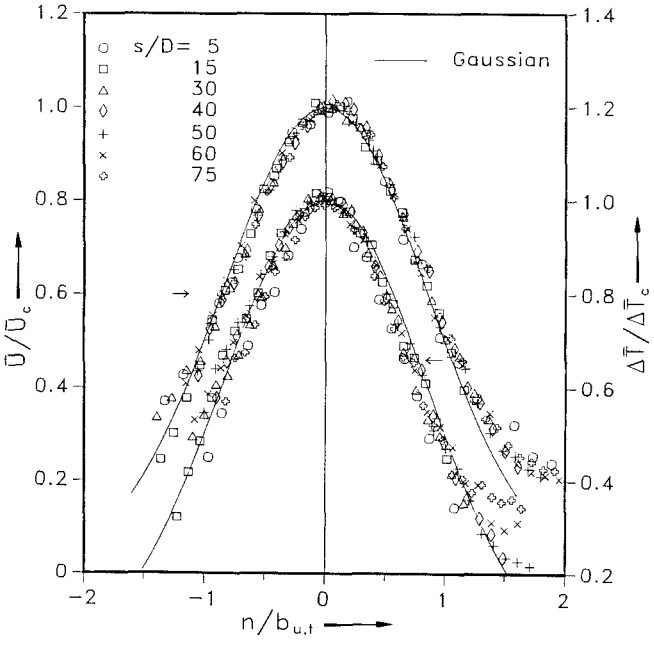

Fig. 4. Self-similar profiles of streamwise mean velocity and mean excess temperature for case C2

The profiles of $\Delta\bar{T}/\Delta T_0$ follow the same dependencies as those described for $\bar{U}/U_0$, except at a fixed θ where excess temperatures were slightly lower for the higher buoyancy (lower Fr) cases. This latter trend is physically more appealing since greater buoyancy is associated with increased production of turbulence and hence more dilution of the jet. Lemieux also observed decreases in $\Delta\bar{T}/\Delta T_0$ as buoyancy was increased at a fixed θ. However, in contrast to the present data, his $\Delta\bar{T}/\Delta T_0$'s were slightly higher in the vertical compared to the inclined jets. In both studies the development of the temperature field proceeds more quickly than that of the velocity field.

The self-similar profiles of $\bar{U}/\bar{U}_c$ versus n/b_u at $s/D=30$ and 60 in Fig. 3a show that the vertical (A2) and inclined jets (B2 and C2) develop identically. Figure 4 presents self-similar profiles of $\bar{U}$ and $\Delta\bar{T}$ for case C2 and is typical of the range of θ's and Fr's tested. This data illustrates both the self-similar and Gaussian nature of the mean velocity and excess temperature.

A test for asymmetry in the lateral distributions of $\bar{U}$ and $\Delta\bar{T}$ was made by folding them about their centerlines. Essentially no asymmetry was found in the profiles of $\bar{U}$, while in case C2 there is some indication of asymmetry in the profiles of $\Delta\bar{T}$ as illustrated in Fig. 4. In this case the spreading of the jet is inhibited on the convex (positive) side which is consistent with the thermal stability of the flow. Lemieux observed asymmetry in his profiles of $\bar{U}$, and to a greater extent, in those of $\Delta\bar{T}$. The more symmetric profiles of the present study suggest that much of the asymmetry in Lemieux's results must be due to his traversing method which locates the upper side of the profiles at a point where more streamwise development has occurred relative to the lower side.

3.3 *Spread rates of velocity and excess temperature*

A mean flow similarity analysis of the plane jet suggests that the velocity and temperature growth rates of the jet's half-widths (db_u/ds and db_t/ds) vary linearly with jet trajectory s, as given respectively by

$$\frac{b_u}{D}=K_u\left[\frac{s}{D}-K_{u_0}\right] \quad \text{and} \quad \frac{b_t}{D}=K_t\left[\frac{s}{D}-K_{t_0}\right] \tag{1}$$

where K_u and K_t are the spread rate constants, and K_{u_0} and K_{t_0} are the geometric origins of the velocity and temperature fields. Table 1 defines the experimental coding and corresponding exit conditions, and summarizes the spreading rates of velocity and temperature as determined by fitting the average of the local half-widths from each side of the jet to the above expressions.

Figure 5 suggests a slight dependence of the spreading rate of velocity on the differences between the series 1 and 2 experiments while no dependence on θ is evident. Although the fitted spreading rates of velocity in Table 1 are generally within the experimental uncertainty of $\approx \pm 5\%$, the actual values do agree with the trend of Fig. 5. Average fits to the data of the series 1 and 2 experiments give velocity spreading rates of 0.126 and 0.137 respectively. Lemieux reports an average spreading rate of 0.128 for all his buoyant results at Re's of 1500 and 1700 indicating no significant dependence on either θ or Fr. Both determinations compare well with some published data on vertical buoyant plane jets [e.g. 0.123 by Reardon (1985) and 0.138 by Bashir and Uberoi 1975], but are larger than the value of 0.11 recommended by Chen and Rodi (1980). However, the effect of low Re needs to be considered.

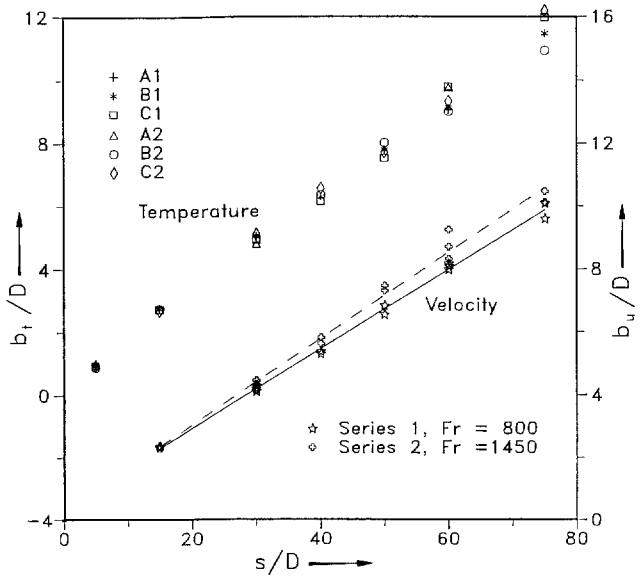

Fig. 5. Spread rates of velocity and excess temperature for vertical and inclined jets

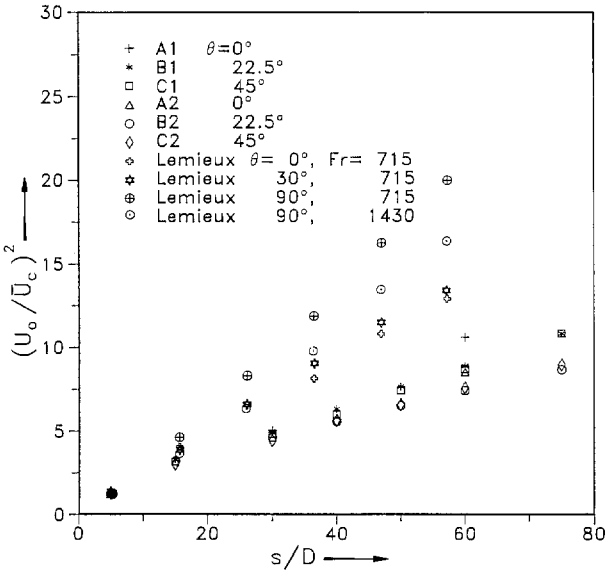

Fig. 6. Variation in the decay of centerline mean velocity with discharge angle

Ray (1986) measured a velocity spreading rate of 0.114 using the present jet apparatus under isothermal conditions with $Re \approx 7000$. Combined with the present results, this indicates a systematic behaviour for Re's between 1900 and 7000. Since the range of Fr studied by Lemieux was nearly identical to the present study but was achieved with a narrower range of Re, it is judged that the increase in the average spreading rate of velocity between series 1 and 2 experiments is due more to the decrease in Re rather than the difference in Fr. This conclusion is supported by the results of Lemieux and Oosthuizen (1984) and also Otugen and Namer (1986) who showed that the rates of spread of velocity decreased from 0.179 to 0.098 as Re increased from 1000 to 6000.

Figure 5 shows that the spread of the temperature field is less dependent on Re and or Fr than the velocity field, but more variable in the far field (e.g. case B2, $s/D \geq 40$). In the near field from $s/D = 5$ to 30, the data for the six cases are nearly coincident, and the fitted spread rates vary between 0.153 and 0.166 with an average value of 0.161. In the far field any definite trend is obscured by the experimental scatter, although in general the rate of spread is lower than in the near field which is opposite to the results of Lemieux. For this reason, the spreading rates of temperature are given for two different ranges in Table 1. The results exhibit no strong dependence on θ, but like velocity, do show a slight increase with decreasing Re and Fr in the region between $s/D = 15$ and 50. The rate of spreading of temperature varies between ≈ 0.14 and 0.16 depending on the region of fit and the exit conditions. This range of values agrees well with the value of 0.14 recommended by Chen and Rodi (1980) for the non-buoyant and intermediate region of vertical non-isothermal plane jets, considering the effects of low Re which tend to increase the rate of spread. Lemieux reports a much higher value of 0.19 for his far field vertical jet data, which he also attributed to the low Re effects. However, for his vertical case given in Table 1, values of 0.132 and 0.136 were determined here, demonstrating the sensitivity of the region of fit in determining these constants. Many other investigators have reported higher values than the one recommended by Chen and Rodi [e.g. Bashir and Uberoi (1975): 0.164, Ramaprian and Chandrasekhara (1983): 0.167 for case MSC2, and Reardon (1985): 0.154].

3.4 Decay of mean centerline velocity and excess temperature

The decay constants of the mean centerline velocity and excess temperature of a non-buoyant plane jet are determined by fitting the data to the self-similar expressions

$$\left(\frac{U_0}{\bar{U}_c}\right)^2 = C_u\left[\frac{s}{D} - C_{u_0}\right] \quad \text{and} \quad \left(\frac{\Delta T_0}{\Delta \bar{T}_c}\right)^2 = C_t\left[\frac{s}{D} - C_{t_0}\right] \qquad (2)$$

where C_u and C_t are the decay rate constants, and C_{u_0} and C_{t_0} are the kinematic origins of the velocity and temperature fields. Figure 6 shows that the decay rates of $\bar{U}_c$ for the present data are much lower than comparable data from Lemieux. In addition, the effect of θ at constant Fr is opposite to that found by Lemieux. The present inclined jet data show a slight increase in the decay rates for the series 1 versus the series 2 experiments while the data of Lemieux (not shown here) shows little effect for $\theta \leq 60°$. However, the decay rate of his horizontal jet at $Fr = 715$ is significantly greater than the equivalent jet at $Fr = 1430$ as shown in Fig. 6. This increase in decay is attributed to the greater buoyancy forces which result in an increase in the turbulence activity of the lower Fr jet.

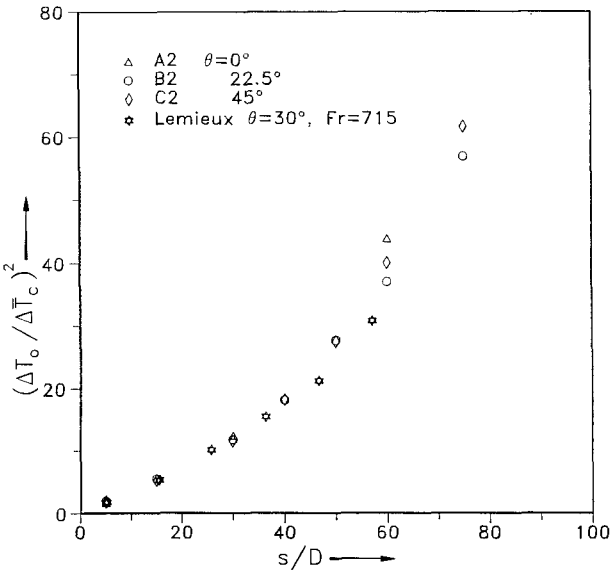

Fig. 7. Variation in the decay of centerline mean excess temperature with discharge angle

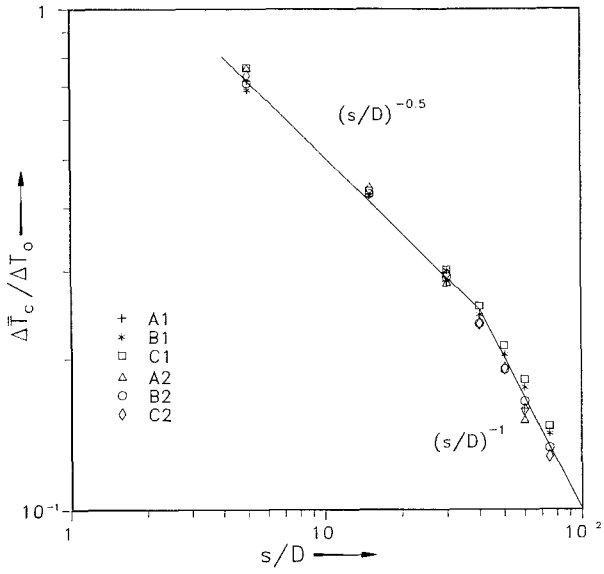

Fig. 8. Jet and plume-like decay regions of centerline mean excess temperature

Ramaprian and Chandrasekhara (1985) argue that the use of U_0 as a scaling velocity does not adequately account for the influence of initial conditions on jet development and thus proposed

$$U_s = (M_\infty/(D-2\phi))^{1/2} \tag{3}$$

where M_∞ is a far field kinematic momentum flux and ϕ is the momentum thickness of the boundary layers on the nozzle walls at the jet exit. It is commonly assumed that momentum is conserved in an isothermal plane jet but measurements have not always shown this (e.g. Hussain and Clark 1977). For this reason the use of M_∞ in the scaling velocity does reduce the scatter in published decay rates of $\bar{U}_c$ (Ramaprian and Chandrasekhara 1985). However, the integrity of the various jet apparatus involved should be better understood so that anomalous influences on the development of the jet can be avoided in future studies.

The decay of the velocity field as plotted in Fig. 6 is essentially linear beyond the first station so the decay constants were fit between $s/D=15$ and 75 as reported in Table 1 for both normalizing velocity scales U_0 (C_u) and U_s (C_u^*). The constants C_u are on average greater for the higher Re and Fr jets (series 1) which is opposite to the data of Lemieux and to the trend identified by Otugen and Namer. However, using the velocity scale U_s reduced the difference between the decay constants C_u^* of the vertical jets to the point that within the experimental uncertainty they are essentially equal. Equal rates of decay of $\bar{U}_c$ for both Re's in this study versus the earlier result of unequal rates of spreading is consistent with the greater sensitivity of the latter to Re in the range around 2000 (Otugen and Namer 1986). Chen and Rodi (1980) recommend $C_u=0.174$ for plane jets which is lower than the corrected constants C_u^* of this study but in agreement with the effects of low Re. The constants C_u and C_u^* were also calculated for Lemieux's vertical jet with $Re=1500$ and found to decrease from 0.211 to 0.178 which agrees with the recommended constant but is not consistent with the present results or the effects of low Re. Presumably, other experimental factors account for the inability of the momentum correction to completely resolve the differences between the two studies.

The decays of $\Delta \bar{T}_c$ for the series 2 data are plotted in Fig. 7 in accord with Eq. (2) along with a single case from Lemieux. A striking agreement exists among the data in the near field. Beyond $s/D=40$ a non-linear decay of $\Delta \bar{T}_c$ occurred in both studies, although more noticably in the present data, indicating a lack of self-similarity. The more quickly diminishing $\Delta \bar{T}_c$ observed for the vertical jet A 2 relative to the inclined jets indicates that this deviation from the expected linear behaviour as given by Eq. (2) is not due to the buoyancy induced curvature. Lemieux's results (not shown here) tend to agree with the above, but like the far field data of series 2 in Fig. 7 are somewhat inconsistent in their behaviour with respect to θ. The faster decay of $\Delta \bar{T}_c$ of the series 2 data ($\varrho_a/\varrho_0=1.25$) relative to the data of Lemieux ($\varrho_a/\varrho_0=1.14$) as shown in Fig. 7 supports the predicted effect of ϱ_a/ϱ_0 on decay rates (Chen and Rodi 1980).

The dimensionless length scale given by Chen and Rodi (1980) as

$$x_1 = Fr^{-2/3}\left(\frac{\varrho_0}{\varrho_a}\right)^{-1/3}\left(\frac{x}{D}\right) \tag{4}$$

places the present data in their intermediate region for $x/D \geq 60$ and 40 for the series 1 and 2 experiments respectively. Thus, in the far field, some deviation from the self-similar decay of $\Delta \bar{T}_c$ as $(s/D)^{-1/2}$ [Eq. (2)] should occur. Figure 8

clearly shows a change in the slope of the decay of $\Delta\overline{T}_c$ in the region beyond $s/D=40$. The slightly earlier change and steeper slope of the series 2 versus series 1 results are consistent with the greater buoyancy forces of the former series. However, the actual decay of $\Delta\overline{T}_c$ is seen to assume a plume-like behavior varying as $(s/D)^{-1}$ which is not expected in the intermediate region. This apparently accelerated transition from jet to plume-like behaviour is likely explained by the specific experimental apparatus and exit conditions used. For example, Chambers et al. (1985) have shown that the more violent near field mixing of the symmetric structures associated with the type of nozzle used here will produce faster jet development than nozzles which induce asymmetric structures.

Following the above observations the decay constants C_t given in Table 1 were calculated for $s/D \leq 30$ where the jet-like behaviour was observed. These constants show similar trends to the constants C_u. On average they are slightly lower for the higher Fr and Re cases A 1, B 1, and C 1, and there is no definite trend with θ. The values of C_t for Lemieux given in Table 1 agree well with the series 1 and 2 averages of 0.382 and 0.405. These decay constants are much higher than the value of 0.25 recommended by Chen and Rodi (1980) but are consistent with the expected influence of Re and ϱ_a/ϱ_0. Lemieux reports average decay constants C_t of 0.51 and 0.32 for all his far field data at Fr's of 715 and 1430 respectively. Ramaprian and Chandrasekhara (1983) found $C_t=0.194$ for the non-buoyant case MSC 2 which is surprisingly low considering the low Re of 1600 and the other results given above.

3.5 Mean transverse velocity

The profiles of mean transverse velocity for the vertical jets exhibit maximum values and locations (n/b_u) of zero velocity which are comparable with other slot jet data (e.g. Krothapalli et al. 1981; Ramaprian and Chandrasekhara 1985). In Fig. 9 profiles of transverse velocity at all downstream stations are plotted for the inclined jets C 1 and C 2. In case C 1 the flow is self-similar out to $s/D=40$, which is consistent with the previous result on the decay of $\Delta\overline{T}_c$, after which, the influence of buoyancy produces an ever increasing shift in the profile such that by $s/D=60$ the entire mean transverse flow is from the convex (lower) to concave (upper) side of the jet. When the buoyancy forces are greatest (case C 2), the advancement to negative transverse flow occurs earlier and results in much larger velocities (about 18% of $\overline{U}_c$), with the maximums located near the jet centerline. Although the near field data of case C 2 appears to be inconsistent, the clear trend of the far field data, in particular on the positive (lower) side of the jet, gives credence to these results. It is noted that on the thermally stable side of the jet (positive n/b_u in the figure) the data points show more uniformity, while on the thermally unstable side, they are more irregular. The transverse velocity gradients apparent in these profiles and the extra buoyancy production terms found in the Reynolds

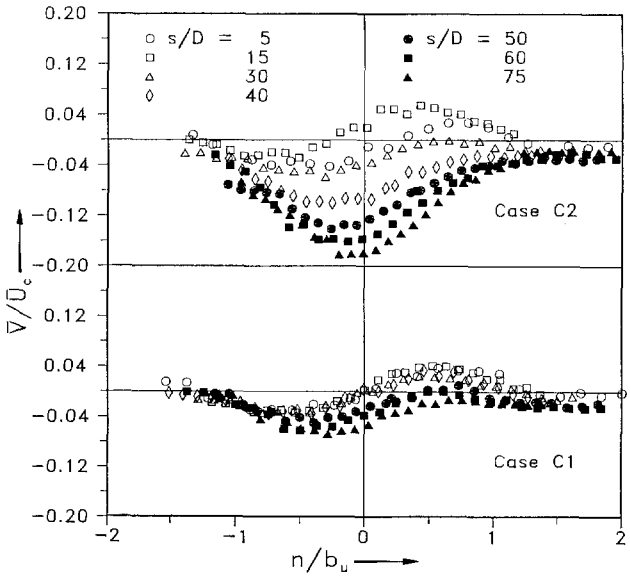

Fig. 9. Profiles of normalized transverse mean velocity for $\theta=22.5°$ (C 1) and $\theta=45°$ (C 2)

stress and turbulent heat flux equations for the present flow (e.g. Bergstrom 1987) would be consistent with buoyancy induced asymmetries occurring in the profiles of transverse normal stress, shear stress, and transverse heat flux. The experimental results of Abdel-Rahman et al. (1988 b) confirm this influence of buoyancy by showing that the above measures of turbulence are enhanced and suppressed on the concave (upper) and convex (lower) sides of the jet respectively.

3.6 Conservation of momentum

In a free non-buoyant turbulent plane jet the momentum flux per unit length M is, in the absence of other forces, a conserved quantity and equal to the source momentum flux per unit length M_0. Assuming the Boussinesq approximation, and that the contribution of turbulence to the total momentum is negligible, then

$$M=\int_{-\infty}^{\infty}\overline{U}^2\,dy=b\,\overline{U}_c^2\int_{-\infty}^{\infty}f^2(\eta)\,d\eta=b\,\overline{U}_c^2\,I \tag{5}$$

where $f(\eta)$ represents the velocity similarity profile which has been shown to be Gaussian and I is the profile integral parameter. Baker et al. (1987) state that integration of experimental data shows that the turbulence quantity $(\overline{u^2}-\overline{v^2})$ accounts for some 5–32% of the total momentum in a fully developed pure jet. They also refer to Seif (1981) who found decreases in M for most published plane jet data even when the turbulence contributions were considered. Ramaprian and Chandrasekhara (1985) conducted a similar survey and noted the confusion introduced by three studies where increases in M occurred. For example, Hussain and Clark (1977) measured up to a 55% increase in M over M_0, and like Ramaprian and Chandrasekhara in their study, attribut-

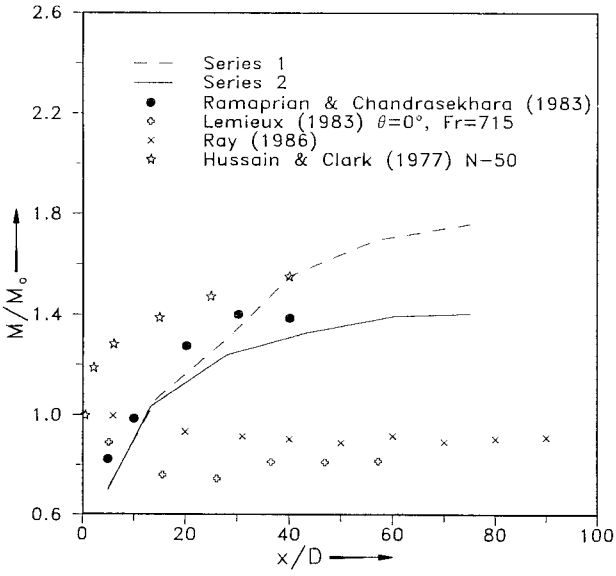

Fig. 10. Variation of momentum flux with streamwise distance

ed the increase to a positive pressure gradient in the axial direction. Both Hussain and Clark and Sfeir (1979) have shown that increases in M depend to some extent on initial conditions, in particular, the nozzle design. Hitchman et al. (1988) found that M/M_0 was significantly reduced when confining end walls were added to the free plane jet configuration. The wide variation of M/M_0 found in the literature, between roughly 0.6 and 1.6, is further evidence of the strong influences of the jet apparatus and experimental conditions on the available data on plane jets.

Figure 10 presents the variation in the momentum flux ratio for the vertical and inclined jet data of this study and, for comparison, results from: Ray (1986; see also Hitchman et al. 1988) for isothermal conditions with $Re=7230$ and wall boundaries similar to this study; Lemieux (1983) for his vertical case with $Fr=715$; Ramaprian and Chandrasekhara (1983) for the non-buoyant case MSC2; and Hussain and Clark (1977) for case N-50 which includes the contribution due to turbulence. In this study, the effect of θ on the conservation of momentum is minimal, following the previous analysis which showed only slight effects on the mean velocity field. However, like the results of Ramaprian and Chandrasekhara and Hussain and Clark, a sharp increase in M occurred in the near field with asymptotic levels 30%–75% greater than M_0 being attained in the far field. These results contrast with those of Lemieux and Ray which gradually decrease in the near field assuming asymptotic levels some 5%–20% less than M_0. The separation of the series 1 and 2 data in Fig. 10 must at this point be attributed to the previously described effects of Re on the spread and decay of the jet.

A review of those investigations in Fig. 10 which show an increase in M revealed that the decay rates of velocity are much lower than those typically found in published data when $\bar{U}_c$ is normalized by U_0. However, no consistent conclusion was reached regarding the nature of these jet apparatus which might explain their similar behaviour. Although Lemieux's jet apparatus has the same slot width and nearly the same aspect ratio as the present one, other differences in design apparently account for the contrasting development of these jets. For example, both use a floor section and confining end walls, but in the present apparatus these features extend 5 times further than in Lemieux's. Besides the differences in wall boundaries, Lemieux used a rectangular plenum with a round edged orifice at one end giving an area contraction of about 10 : 1, while a much larger settling chamber was used here, with a smoothly reducing nozzle based on a cosine curve producing an area contraction of 40 : 1. Regrettably, the available experimental data is not sufficient to resolve the discrepancies between these studies.

Hussain and Clark's jet issued from a relatively large floor but unlike the other studies represented in Fig. 10 was otherwise unbounded. Their evidence that a favourable pressure gradient in the axial direction produced the measured increase in M needs to be pursued in light of the many studies where decreases in M were found. More specifically, the reason that both an increase and decrease in M has occurred in the present jet apparatus, albeit at different Re's and slightly altered wall boundaries, needs to be understood.

4 Conclusions

There is little experimental data on heated plane jets with buoyancy induced curvature. The experimental results of the present study indicate how buoyancy induced curvature affects the mean flow characteristics of a heated plane turbulent jet in the non-buoyant and intermediate regions. Comparisons with a similar study illustrate the potential sensitivity of the results to experimental technique and apparatus design.

The spread rates of the velocity and temperature fields, along with the decay rate of centreline velocity, depend not only on the initial Re and Fr numbers as in heated jets without curvature, but also on the amount of buoyancy induced curvature present. Buoyancy induced curvature appears to have little effect on the shape of the mean streamwise velocity and temperature profiles as they are found to be symmetric and self-similar within experimental uncertainty. As one might expect, transition from the non-buoyant region of the jet to the intermediate region occurs more quickly as buoyancy induced curvature is increased.

The most significant effect of the competing influences of buoyancy and curvature on the mean flow characteristics is due to buoyancy, as seen in the increasingly asymmetric profiles of mean transverse velocity. The transverse velocity gradients indicated by these profiles are consistent with the asymmetries in the profiles of transverse normal stress, shear stress, and transverse heat flux as reported by Abdel-Rahman et al. (1988b).

Acknowledgements

The authors gratefully acknowledge the financial support of the Natural Sciences and Engineering Research Council of Canada.

References

Abdel-Rahman, A.; Hitchman, G. J.; Slawson, P. R.; Strong, A. B. 1988 a: An X-array hot-wire technique for heated turbulent flows of low velocity. J. Phys. E, in press

Abdel-Rahman, A.; Hitchman, G. J.; Strong, A. B.; Slawson, P. R. 1988 b: Turbulence measurements in a plane air jet with buoyancy induced curvature. Exp. Thermal Fluid Science, in press

Abdel-Rahman, A. 1987: An experimental investigation of a buoyant turbulent plane jet with streamline curvature. Ph.D. Thesis. Ontario: University of Waterloo

Abdel-Rahman, A.; Tropea, C.; Slawson, P.; Strong, A. 1987: On temperature compensation in hot-wire anemometry. J. Phys. E 20, 315–319

Abraham, G. 1963: Jet diffusion in stagnant ambient fluid. Delft Hyd. Lab. Pub. 29. Holland: Delft

Abraham, G. 1965: Horizontal jets in stagnant fluid of other density. J. Hydraul. Div. ASCE 91, 139–154

Anwar, H. O. 1969: Experiment on an effluent discharging from a slot into stationary or slow-moving fluid of greater density. J. Hydraul. Res. 7, 411–430

Bashir, J.; Uberoi, M. 1975: Experiments on turbulent structure and heat transfer in a two-dimensional jet. Phys. Fluids 18, 405–410

Baker, C. B.; Maffe, A. J.; Taulbee, D. B. 1987: An analysis of the two-dimensional turbulent buoyant jet. ASME HTD-70, 24th Nat Heat Transfer Conference and Exhibition. Pittsburgh: New York: ASME

Bergstrom, D. J. 1987: A computational study of plane buoyant free jets using algebraic stress-flux models. Ph.D. Thesis. Ontario: University of Waterloo

Bradshaw, P. 1973: Effects of streamline curvature on turbulent flow. AGARDograph No. 169

Bruun, H. H. 1972: Hot-wire data correction in low and high turbulence intensity flows. J. Phys. E 5, 812–818

Bruun, H. H.; Tropea, C. 1985: The calibration of inclined hot-wire probes. J. Phys. E 18, 405–413

Cederwall, K. 1971: Buoyant slot jets into stagnant or flowing environments. W. M. Keck, California Inst. Technol., Report No. KH-R-25

Chambers, A. J.; Antonia, R. A.; Browne, L. W. B. 1985: Effect of symmetry and asymmetry of turbulent structures on the interaction region of a plane jet. Exp. Fluids 3, 343–348

Champagne, F. H.; Sleicher, C. A.; Wehrmann, O. H. 1967: Turbulence measurements with inclined hot-wires. Part 1. Heat transfer experiments with inclined hot-wire. J. Fluid Mech. 28, 153–175

Chan, T. L.; Kennedy, J. F. 1972: Turbulent non-buoyant or buoyant jets discharged into flowing or quiescent fluids. IIHR Report No. 140, University of Iowa

Chen, C. J.; Rodi, W. 1980: Vertical turbulent buoyant jets – A review of experimental data. Oxford: Pergamon Press

Collis, D. C.; Williams, M. J. 1959: Two-dimensional convection from heated wires. J. Fluid Mech. 6, 357–384

Fan, L.; Brooks, N. H. 1969: Numerical solutions of turbulent buoyant jet problems. W. M. Keck, California Inst. Technol., Report No. KH-R-18

Hitchman, G. J.; Strong, A. B.; Slawson, P. R.; Ray, G. D. 1988: The turbulent plane jet with and without confining end walls. AIAA J., in press

Hussain, A. K. M. F.; Clark, A. R. 1977: Upstream influence on the near field of a plane turbulent jet. Phys. Fluids 20, 1416–1426

Krothapalli, A.; Baganoff, D.; Karamcheti, K. 1981: On the mixing of a rectangular jet. J. Fluid Mech. 107, 201–220

Lemieux, G. P. 1983: An experimental study of the effects of Reynolds number and buoyancy upon the structure of inclined turbulent two-dimensional jets. Ph.D. Thesis. Kingston, Ontario: Queen's University

Lemieux, G. P.; Oosthuizen, P. H. 1984: Experimental study of the behaviour of plane turbulent jets at low Reynolds numbers. AIAA 17th Fluid Dynamics, Plasma Dynamics, and Lasers Conference. Snowmass, Colorado

Otugen, M. V.; Namer, I. 1986: The effect of Reynolds number on the structure of plane turbulent jets. AIAA 24th Aerospace Sciences Meeting, Reno, Nevada

Pelfrey, J. R. R.; Liburdy, J. A. 1986: Effect of curvature on the turbulence of a two-dimensional jet. Exp. Fluids 4, 143–149

Ramaprian, B. R.; Chandrasekhara, M. S. 1983: Study of vertical plane turbulent jets and plumes. IIHR Rep. No. 257, University of Iowa

Ramaprian, B. R.; Chandrasekhara, M. S. 1985: LDA measurements in plane turbulent jets. Trans. ASME 107, 264–271

Ray, G. D. 1986: Characteristics of a vertical isothermal plane jet. MASc. Thesis. Ontario: University of Waterloo

Reardon, J. T. 1985: An experimental investigation of the turbulence structure of a heated plane jet. Ph.D. Thesis. Ontario: University of Waterloo

Seif, A. A. 1981: Higher order closure model for turbulent jets. Ph.D. Thesis. State University of New York at Buffalo

Sfeir, A. A. 1979: Investigation of three-dimensional turbulent rectangular jets. AIAA J. 17, 1055–1060

Received March 27, 1989